IAC-07- E2.2.07

LOW-THRUST TRAJECTORIES DESIGN FOR THE EUROPEAN STUDENT MOON ORBITER MISSION

Camilla Colombo
University of Glasgow, UK
e-mail: ccolombo@eng.gla.ac.uk

Daniel Novak
University of Glasgow, UK
e-mail: dnovak@eng.gla.ac.uk

Jeannette Heiligers
Delft University of Technology, the Netherlands
e-mail: m.j.heiligers-lr@student.tudelft.nl

ABSTRACT

The following paper presents the mission analysis studies performed for the phase A of the solar electric propulsion option of the European Student Moon Orbiter (ESMO) mission. ESMO is scheduled to be launched in 2011, as an auxiliary payload on board of Ariane 5. Hence the launch date will be imposed by the primary payload. A method to efficiently assess wide launch windows for the Earth-Moon transfer is presented here. Sets of spirals starting from the GTO were propagated forward with a continuous tangential thrust until reaching an apogee of 280,000 km. Concurrently, sets of potential Moon spirals were propagated backwards from the lunar orbit injection. The method consists of ranking all the admissible lunar spiral-down orbits that arrive to the target orbit with a simple tangential thrust profile after a capture through the L_1 Lagrange point. The 'best' lunar spiral is selected for each Earth spiral. Finally, comparing the value of the ranking function for each launch date, the favourable and unfavourable launch windows are identified.

1. INTRODUCTION

Finding the optimal trajectory for missions employing low-thrust propulsion is mathematically and computationally a complex problem. Moreover, when designing trajectories for real missions, many constraints arising from the scientific, technological or operational requirements have to be taken into account. The case of the European Student Moon Orbiter (ESMO), a low-cost student-designed and operated spacecraft, is no exception.

ESMO is a mission proposed by the Student Space Exploration & Technology Initiative (SSETI), an association cooperating closely with the European Space Agency (ESA) Education department, and it was approved for phase A feasibility study.

If launched in 2011, ESMO will be the first lunar mission to be entirely designed by students belonging to ESA's Member and

1

Cooperating States. Its primary objective (Outreach mission) is to place an orbiter on a stable orbit around the Moon and to send back images acquired through a high-resolution narrow angle CCD camera (NAC) for optical imaging of lunar surface characteristics. The selected target on the lunar surface is the South Pole [1][2]. As a secondary objective (Science mission), some scientific experiments shall be performed from a 100 km science orbit. A nano-satellite, Lunette, would be responsible for the gravity field mapping via the Doppler Effect. In order to minimise costs, the spacecraft will be an auxiliary payload fitted on the ASAP (Ariane Structure for Auxiliary Payloads) ring of an Ariane 5 launcher.

The Space Advanced Research Team at the University of Glasgow was selected as the primary team for the ESMO mission analysis and design. For each one of the two missions, two types of transfers were studied, using different propulsion systems: one based on a chemical propulsion, and the other on a low-thrust solar electric propulsion scheme. The work described in this paper focuses on the methodology and results for the design of an Earth-Moon trajectory using low-thrust electric propulsion. The increasing importance of low-thrust trajectories in the last few years is underlined by successful missions such as Deep Space One [3] and SMART-1 [4][5]. The latter, launched in 2003 using low-thrust ion propulsion, was the first ESA mission to orbit the Moon. The optimisation of the lunar transfer involved a phasing strategy using a sequence of short-thrusting manoeuvres to reposition the spacecraft before lunar capture, in order to maximise the benefits of lunar resonances [4]. This is similar to the approach used in the mission design of BepiColombo [6]; the operational orbit around Mercury was propagated backwards to determine the optimal point of capture by the gravity field of Mercury.

Other studies dealt with electrical transfers to near-Earth objects [7][8], to halo orbits [9][10], and with multiple gravity assist interplanetary missions [11]. In fact low-thrust propulsion has become a real alternative to chemical propulsion, since it is able to offer a long duration thrust with a very high specific impulse. The efficiency of an electrical propulsion system can be up to 60-70%. This means that the total amount of Δv can be much greater than the one given by chemical engine, with the same amount of propellant. The downside is that a low-thrust trajectory usually requires a longer transfer time to reach the target. In addition, the design of an optimal low-thrust trajectory represents a challenge for mission analysts [12][13].

Direct and indirect approaches have been developed, in order to find optimal or sub-optimal low-thrust trajectories. A shape based method has been proposed by Petropoulos et al. [14][15] and an inverse shape based technique by De Pascale and Vasile [16]. Different other techniques have been developed for low thrust trajectories in the three-body problem (see for example [17] for further details).

For the design of trajectory in the Earth-Moon system, the Circular Restricted Three Body Problem (CRTBP) is often applied to analyse the motion of a spacecraft subject to the gravitational pull of two bodies. However, the design is often focused on trajectories using impulsive transfers. Kluever and Pierson [18], and Herman and Conway [19] both investigated using low-thrust propulsion within the CRTBP with the aim of optimising propellant mass.

In this work, the trajectory design is extended to the four-body, unrestricted model. The prime objective is to identify favourable launch windows. As the spacecraft is an auxiliary payload, the mission must be designed with a flexible date of launch anytime within a 3-year period. Due to size of the search space, a method was developed to effectively identify and assess of a large number of launch opportunities in a short amount of time.

The present paper is structured in the following way: the overall design strategy is explained first, then the detailed description of the methodology adopted for generating the up- and down-spirals and for assessing the transfer between them is given. Finally, one optimised trajectory starting in an unfavourable launch window will be presented and analysed for both the Outreach and the Science mission.

2. DESIGN STRATEGY

The ESMO mission requires an efficient and reliable preliminary design of the low-thrust Earth-Moon transfers, for 365 possible launch dates. In other terms, it is required to find the optimal thrust profile for a transfer orbit, which links an initial Earth-centred orbit to a Moon-centred one. Performing such an optimisation for each launch date is technically feasible but may require a lot of time and computational power. An alternative approach is proposed here: it turned out to be suitable to get preliminary results in a short time, in line with the phase A requirements of the ESMO mission [1].

A complete transfer trajectory to the Moon is composed of three phases: a spiralling-up segment from the Earth, the lunar capture, and spiralling-down segment at the Moon. The three legs were designed independently, and then linked together. Among them, the delicate part is to find the best 'keyhole' between the Earth and the Moon that leads to a capture.

For the ESMO mission, the spiralling-up phase is the longest one. Furthermore, operational reasons require shortening this phase as much as possible. A continuous, tangential thrust profile was then selected, as this guarantees the fastest way to spiral-up. At the same time, it does not require any optimisation, but just a forward propagation in time of the trajectory.

With the same considerations, the spiralling-down to the Moon can be computed, adopting a continuous and tangential thrust profile. Again, no optimisation is needed for the injection of the spacecraft into the target lunar orbit. A backward propagation from the target orbit was performed, with a stopping condition.

Once the spiralling-up and the spiralling-down phase have been fixed, a lunar capture has to be designed, such that all the legs can be linked together. The capture phase is not always feasible, especially if the arrival conditions at the target lunar orbit (arrival time and orbital elements) are highly constrained, unless additional manoeuvres are inserted between the capture and the start of the spiralling-down phase.

If, on the contrary, degrees of freedom in the arrival conditions exist, they can be used to generate sets of potential spiralling-down trajectories. In this way, the portion of the lunar transfer during which the thrust profile is variable is significantly reduced to a couple of Earth-centred orbits, which is a much easier problem to tackle.

This is the case of the ESMO lunar operational orbit (LOO): due to mission requirements, the lunar target orbit has two degrees of freedom: the right ascension of the ascending node (RAAN) and the time of arrival. It is then possible to generate a set of lunar spirals, varying the parameters with a degree of freedom.

One Earth spiral for each possible launch date is also generated. Then, for each one of the Earth spirals, a ranking of the lunar spirals is done, and the best one is selected. Finally, the values of the ranking function of the selected Moon spirals are compared for all launch dates and the worst launch windows are identified in this way. Once a Moon spiral has been selected for each Earth spiral, the subsequent optimisation of the whole transfer, including the capture phase, is done with DITAN (Direct Interplanetary Transfer Analysis), a local optimiser for low-thrust trajectories [20].

This paper presents the method adopted to design a first guess solution for each launch date.

2.1. *Earth spiralling-up phase*

The spiralling-up phase around the Earth is done by propagating the equations of motion forward in time, considering a continuous tangential thrust, except when in the umbra of the Earth. It starts at perigee after seven days of Launch and Early Operations Phase (LEOP) and ends when the spacecraft reaches an apogee of 280,000 km. The orbital parameters of the GTO [21] into which ESMO will be injected are given in Table 1. The forces taken into account in the equations of motion (in addition to the thrust) are the gravitational attraction of the Earth, the Moon and the Sun, as well as the perturbation due to the J_2 term originating from the oblateness of the Earth. The mass of the spacecraft is governed by the following equation:

$$\dot{m} = -\frac{T}{g_0 I_{sp}} \qquad (1)$$

where $\dot{m}$ is the time-derivative of the spacecraft mass, T is the amplitude of the thrust vector, g_0 is the standard free-fall acceleration and I_{sp} is the specific impulse of the engine. The spacecraft is equipped with a T5 gridded ion thruster (see Table 2). The thrust can be switched either on and off, with no thrust produced during eclipse time.

The propagation is stopped once the spacecraft's apogee reaches 280,000 km.

Table 1: Orbital elements of the initial GTO

Description	Value
Altitude of perigee	250 km
Altitude of apogee	35950 km
Inclination	7°
Longitude of first descending node with respect to Greenwich	0°
Argument of perigee	178°

Table 2: Physical properties of the solar electric propulsion system

	Outreach option	Science option
Thrust	20 mN	
Isp	3250 s	
Initial mass of the spacecraft	180 kg	200 kg

Fig. 1 to Fig. 6 show - for both Outreach and Science mission - the times of flight, the propellant consumptions, the perigee radii, the inclinations, the arguments of perigee and the RAANs, for all the launch opportunities throughout 2011.

The graphs of the time of flight (Fig. 1), the propellant consumption (Fig. 2), and the perigee radius (Fig. 3) show common patterns, i.e. peaks and troughs. This is explained considering that, when the apogee reaches 280,000 km, if the perigee is higher than a reference value, then more time is spent raising the perigee, and therefore more propellant is consumed. It can be noticed that in general the peaks and valleys recur in periods of slightly below 30 days, close to the Moon's period : in fact, although there are many lunar periods passing by during the spiralling-up phase, the phasing of the launch date within a lunar period makes the spacecraft more prone to enter into slight resonances with the Moon, influencing certain parameters more intensely.

It is also worth noting that although there are peaks and troughs in the propellant consumption (see Fig. 2), the maximum difference between the best and worst cases is only around 350 g of propellant and 7 days of flight time for both missions.

General tendencies on a longer time scale can also be observed. The argument of perigee (Fig. 5) always increases. Indeed, it migrates from an initial 178° at GTO to a value between 200° and 290°. It is clear that the shape of the curve in Fig. 5, representing the arguments of perigee, is exactly the opposite of that of the inclinations, in Fig. 4. The perturbations affecting the right ascensions of the ascending nodes (Fig. 6) are less erratic.

There is also a critical period in the propellant consumption mass (Fig. 2) equal to half a year. The origin of this is the alignment of the line of nodes of the initial GTO with that of the Moon. Indeed, since the Moon's line of nodes is relatively constant over the year, only the line of nodes of the GTO is varying, uniformly prescribing a full circle. The two lines are aligned every 180°, i.e. every six months. This geometrical property is one of the key issues affecting the assessment of the most unfavourable launch date.
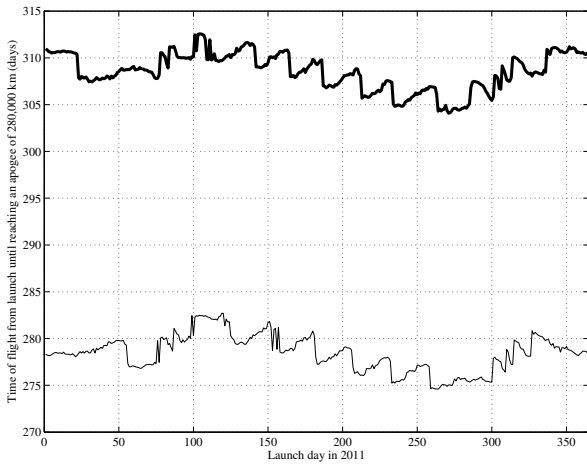
Fig. 1: Time of flight to reach an apogee of 280,000 km (thin line: Outreach, bold line: Science).
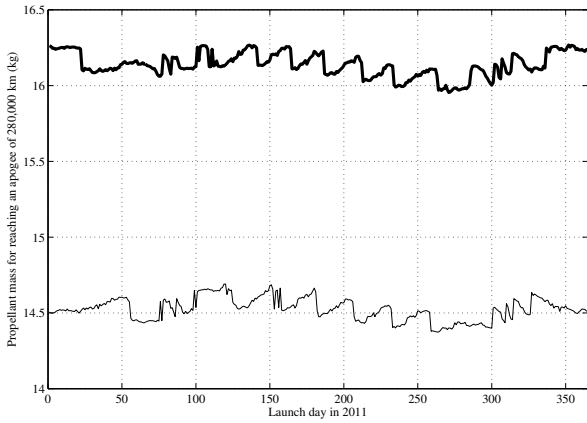

Fig. 2: Propellant consumption to reach an apogee of 280,000 km (thin line: Outreach, bold line: Science).
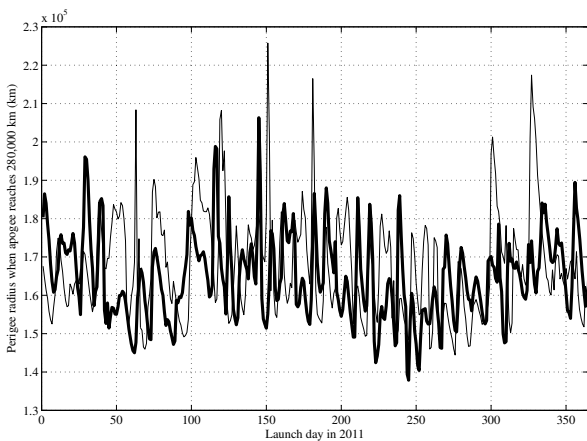

Fig. 3: Perigee radius when the apogee reaches 280,000 km (thin line: Outreach, bold line: Science).
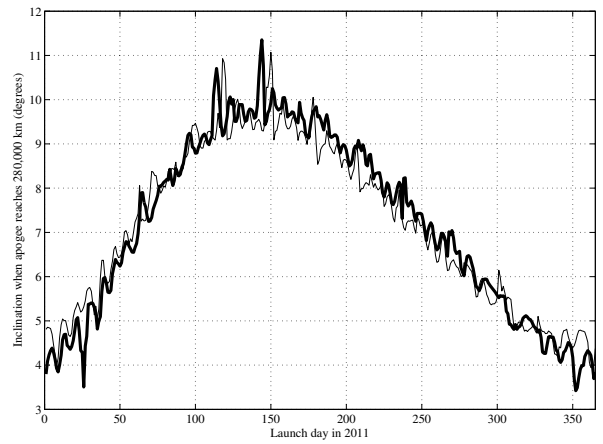

Fig. 4: Inclination when the apogee reaches 280,000 km (thin line: Outreach, bold line: Science).
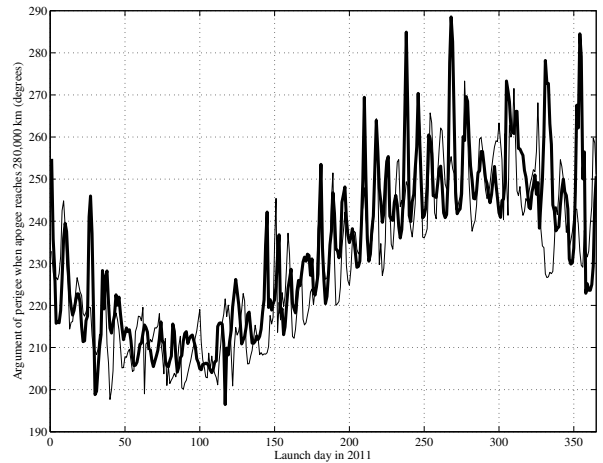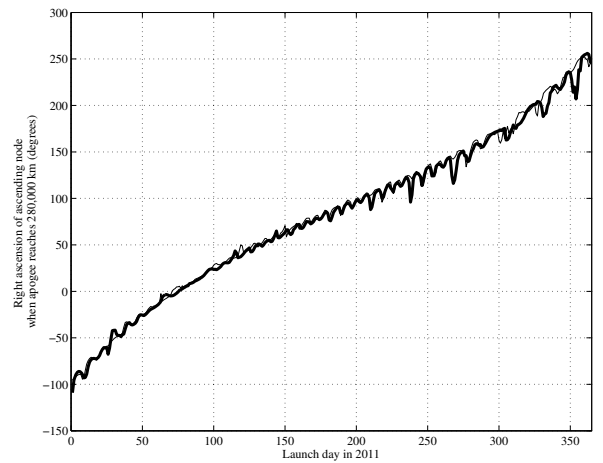

Fig. 5: Argument of perigee when the apogee reaches 280,000 km (thin line: Outreach, bold line: Science).

Fig. 6: RAAN when the apogee reaches 280,000 km (thin line: Outreach, bold line: Science).

5

2.2. *Moon spiralling-down phase*

Outreach mission

As for the Earth spiral, the Moon spiral is generated considering continuous tangential thrust, except in eclipses, integrating backward in time. The thrust vector is opposite to the velocity vector in this case, since the objective is to lower the semi-major axis. The propagation stops when the aposelenium radius reaches 60,000 km, an altitude high enough to have a Jacobi integral allowing an escape from the Moon. At this point the thrust is cut off and the trajectory is further propagated backward for 10 days, at which point the lunar capture is expected to take place.

The initial mass of the backward propagation, in this case, is unknown: this is the mass of the spacecraft at the Lunar Outreach Orbit (LOO), which depends on the previous part of the trajectory. This mass can only be estimated in this part of the study. The value was set to 156 kg for the Outreach mission and 174 kg for the Science mission: these values turned out to be not far from the final mass budget derived later in this work, and corresponding to a total propellant consumption of respectively 24 kg and 26 kg.

The orbital elements of the target lunar orbit are reported in Table 3 for each mission. The inclination, the altitude of periselenium and the argument of periselenium are imposed by the mission requirements, the best altitude of aposelenium is found through stability analysis, so the remaining orbital element, the right ascension at arrival is a free parameter which can be chosen either for science or for transfer feasibility.

Thus a complete catalogue of lunar spirals was created, indexed by the date and right ascension at the beginning of LOO.

Table 3: Lunar Injection orbits

	Outreach	Science
Semi-major axis	3586 km	1856 km
Inclination	90°	90°
Eccentricity	0.4874	0.0092
Periselenium altitude	100 km	100 km
Aposelenium altitude	3600 km	135 km
Argument of the periapsis	293°	90°
RAAN	free	free

Science mission

The strategy used to compute the Moon spiralling phase for the Science mission is similar to the Outreach mission. In this case, though, the thrust is continuous only when the altitude of periselenium is above 575 km. At lower altitudes, the thrust is still tangential and opposite to the velocity vector, but applied in proximity of the periselenium. The reason is that the operational Science mission orbit is quasi-circular, and thus the need to change its eccentricity. In particular, considering moving forward in time, the eccentricity needs to be decreased to reach the value of the target orbit (i.e., close to zero).

The condition on when to thrust is derived from Gauss' variational equation for the value of the eccentricity [22]:

$$\frac{de}{dt} = \frac{2}{v}\left(e + \cos(f)\right)a_t \qquad (2)$$

where f is the instantaneous true anomaly, v is the value of the velocity and a_t is the value of the local acceleration due to the thrust (in this specific case it will have a negative value). Hence e will decrease if $\cos(f) > -e$.

Thrusting around the periselenium with such a strategy has the effect of reducing the aposelenium radius, as well as the periselenium radius. With an initial value of 575 km for the altitude of periselenium, the eccentricity will reach a value very close to zero together with a periselenium altitude of 100 km.

2.3. *Spiral selection*

The objective is to find for each Earth spiral, the best lunar spiral in the catalogue of possible arrival dates and RAANs at LOO.

When further propagating the lunar spirals backwards for 10 days, without any thrust, it can be noted that some trajectories escape through the L_2 Lagrange point of the Earth-Moon system, due to the third body perturbations of the Earth. These lunar spirals cannot be accepted, since it would require more time and propellant to reach the farther side of the Moon. The spirals kept as possible candidates for further study are plotted in Fig. 7, indexed by their arrival date and right ascension at the beginning of LOO; these ones escape through L_1 within 10 days of coast arc.

For each arrival date, the set of spirals allowing an escape through L_1 are not spread in the whole interval of RAAN; rather, they have values of RAAN in an interval, which seems to translate with the day of arrival, and shows a periodicity of 27 days, equal to the Earth-Moon system period.
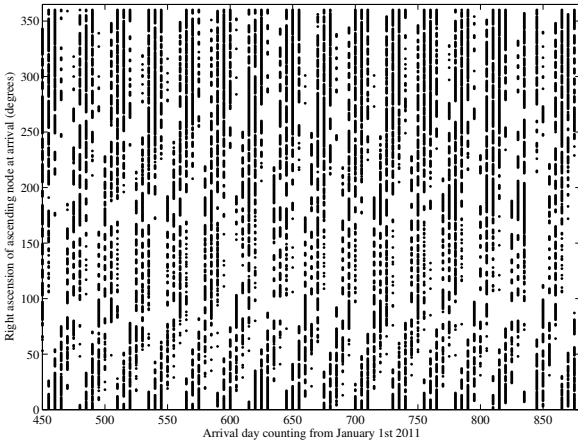
Fig. 7: Moon spirals that can be linked through L_1 to the Earth sphere of influence within 10 days of coast arc. Science mission.

It is worth to note that the set of potential spiral candidates includes also weak stability captures; moreover, while propagating the trajectory backwards without thrust, the spacecraft may perform non-Keplerian loops or revolutions around the Moon before being captured by the Earth's gravity field. These types of transfers are not allowed, since they require stringent navigation: in fact, because

of their instability, deviating even slightly from the ideal trajectory may result in completely altered arrival conditions.

The association of each Earth spiral with a Moon spiral plays an important role in the whole method, as from this depends the possibility to link the two phases.

Essentially, given an Earth spiral, the problem is to find a way to detect the best Moon spiral. Since the final objective is to find an orbit linking two state vectors belonging to two geocentric orbits – the end of the Earth spiral with the beginning of the Moon spiral – the most natural way to rank the Moon spirals is by comparing the orbital elements of their starting point with the one at the end of the given Earth spiral. The process is repeated for each Earth spiral.

A ranking function for each Earth spiral was defined to this aim:

$$R_{D_{launch}}\left(D_{arrival}, \Omega_{arrival}\right) = \frac{5 \cdot 10^{-8}}{km^2}\left(r_{pM} - r_{pE}\right)^2$$
$$+ \frac{2}{deg}\left(i_M - i_E\right) \qquad (3)$$
$$+ \frac{5 \cdot 10^{-3}}{deg^2}\left(\Omega_M - \Omega_E\right)^2$$

where i_E and i_M are the inclinations at the end of the Earth spiral and at the beginning of the Moon spiral respectively, Ω_E and Ω_M are the corresponding anomalies of the ascending node, r_{pE} and r_{pM} are the perigee radii.

The choice of the coefficients was made in order to weigh properly the difference in the orbital parameters. The inclination is taken in the interval [0, 90] deg, and the right ascension is in [-90, 90] deg. As an example, a difference of 10,000 km in perigee radius contributes with 5 units, a difference of 10 deg in inclination contributes with 20 units and a difference of 60 deg of the RAAN contributes with 18 units.

The reason for which the perigee radius difference $(r_{pM} - r_{pE})$ is present in the ranking function is that it would require less energy to raise only the apogee, while maintaining the perigee quasi-constant.

The ranking function in Eq. (3) is an intuitive guess, but it is the simplest and most natural way to start the analysis. Ideally, the ranking function should introduce other orbital

elements, include coupling terms, and eventually take into account phasing properties leading to resonance.

In addition to the ranking, a constraint was imposed on the difference between the time at the end of the Earth spiral and the time at the beginning of the Moon spiral. This difference was constrained to be between 70 and 120 days, in order to allow enough time to raise the apogee, change the inclination and adjust all the other orbital parameters to those of the target. The time difference was upper bounded to avoid a long transfer time, without limiting excessively the number of Moon orbits to choose from.

3. **RESULTS AND ANALYSES**

Following the proposed approach, a first guess transfer was calculated for each launch date in the year 2011. Afterward, by comparing the value of the ranking function, the bad and good launch windows were identified, as shown in Fig. 8. The overall trend line increases in correspondence of the unfavourable launch dates – in terms of transfer optimality – in mid summer and mid winter, and decreases for launch opportunities in mid spring and mid autumn. The reason of a high value of the ranking function is the non-alignment of the line of nodes of the two state vectors to be linked, at the end of the Earth spiral and at the beginning of the Moon spiral-down respectively.
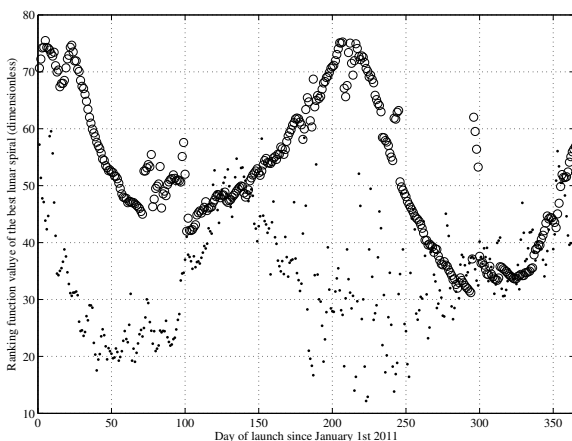
Fig. 8: Value of the ranking function for the optimal transfers for each launch date (Dots: Outreach mission, circles: Science mission).

Fig. 9 links the launch dates with the corresponding arrival dates at the Moon. It is worth to note that for a certain range of launch dates, the arrival date is the same and therefore the selected Moon spiral too. This is due to the constraint on the time difference between the end of the spiral-out and the beginning of the capture. Therefore the conditions at this point represent "keyholes" that the orbit should intersect.
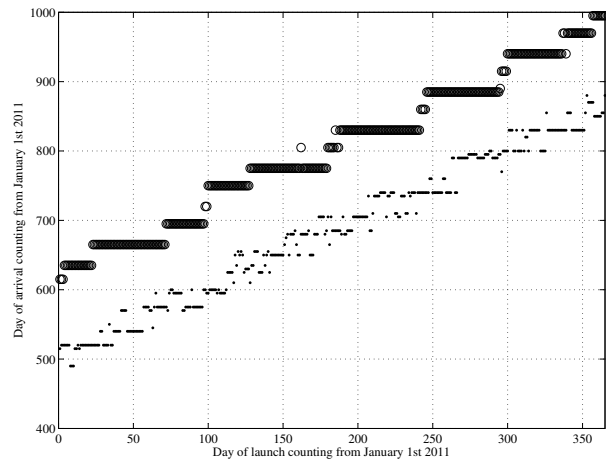

Fig. 9: Optimal arrival date corresponding to every launch date (Dots: Outreach mission, circles: Science mission).

The solutions with the same arrival date differ for time of flight, as is highlighted in Fig. 8.
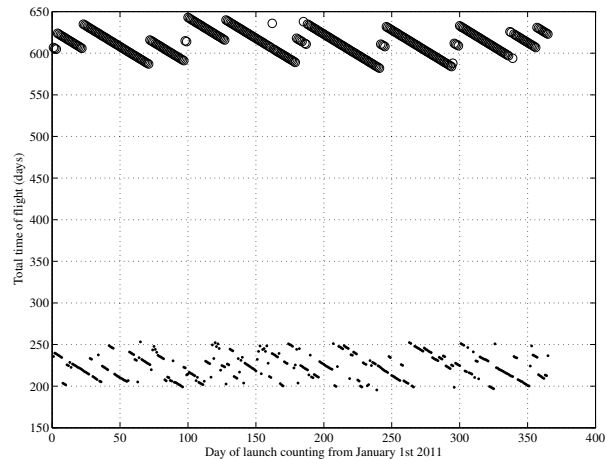

Fig. 10: Total time of flight for every date of launch (Dots: Outreach mission, circles: Science mission).

Once a launch date had been selected for further investigation, the low-thrust phasing leg was locally optimised, minimising the

8

propellant consumption, with the software DITAN. Two solutions for each mission were selected, launching in the two unfavourable windows, in order to have a conservative design.

One full low-thrust trajectory for each mission is here presented.

Outreach trajectory

The trajectory analysed for the Outreach mission launches on January 9th 2011 and is represented in Fig. 11:
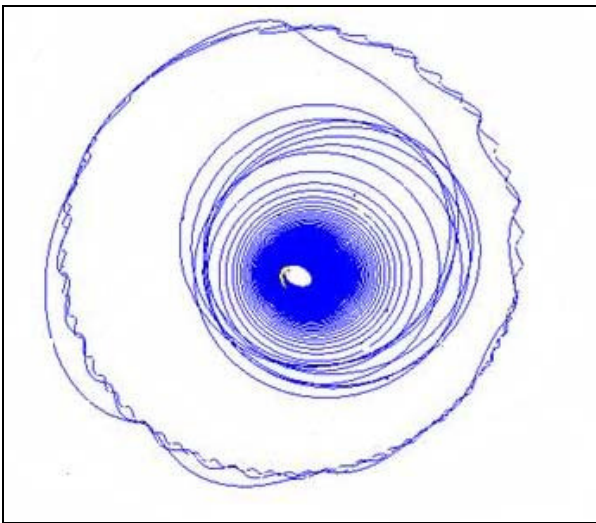

Fig. 11: Full trajectory for the Outreach mission projected on the plane of motion of the Earth-Moon system.

During the phasing leg, the variation of orbital parameters is entirely due to the thruster, the Moon barely influences the orbital elements. Once the apogee reaches 280,000 km, the perigee is kept constant while the apogee is raised gradually. Concurrently the inclination and the right ascension are adjusted to the target values to inject the Moon spiral.

The evolution of the inclination and the right ascension during the phasing leg are shown in Fig. 12 and Fig. 13 respectively.
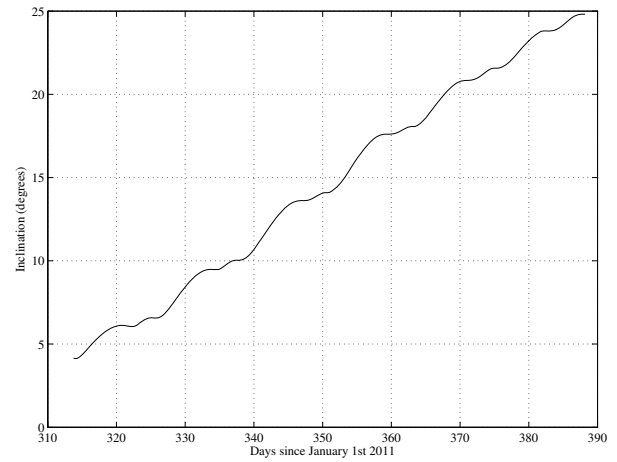
Fig. 12: Evolution of the inclination during the phasing leg for the Outreach mission.
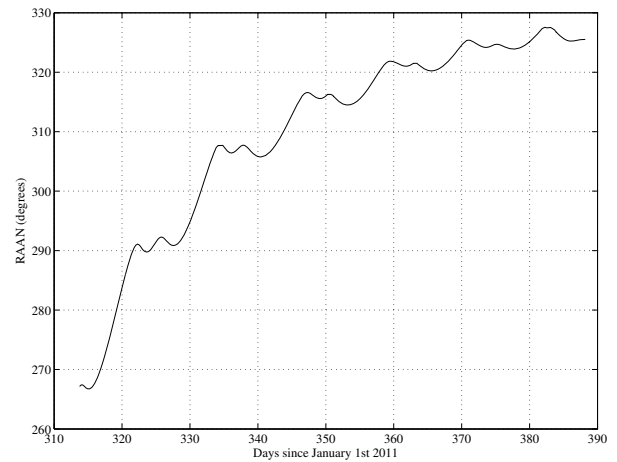

Fig. 13: Evolution of the RAAN during the phasing leg for the Outreach mission.

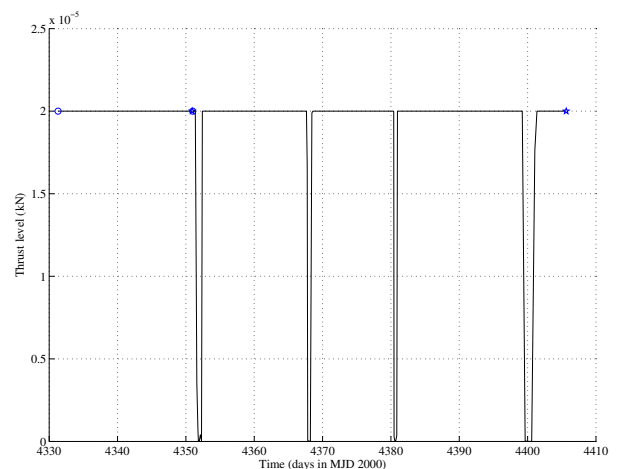Fig. 14 shows the amplitude of the thrust vector during the phasing leg for the Outreach mission.

Fig. 14: Amplitude of the thrust vector during the phasing leg for the Outreach mission.

9

The out-of-plane components of the thrust vector are important; in fact they are responsible for the change in inclination. Fig. 22 contains the elevation angle of the thrust vector, whereby Fig. 23 shows the azimuth angle.
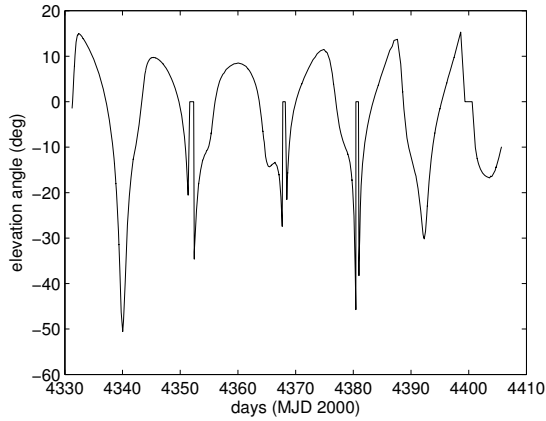

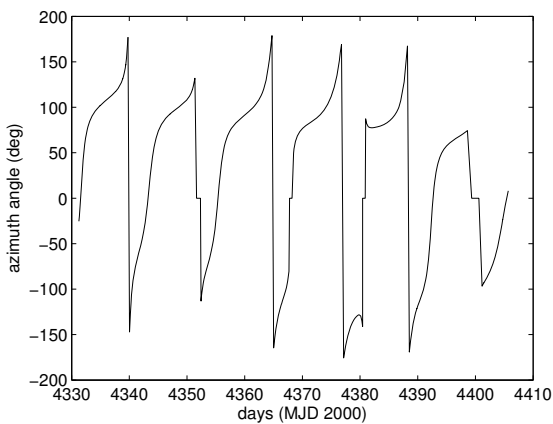Fig. 15: Elevation angle of the thrust vector during the phasing leg for the Outreach mission.

Fig. 16: Azimuth angle of the thrust vector during the phasing leg for the Outreach mission.

As final step of the trajectory design, the lunar spiral-down is propagated forward, with the actual value of the mass at the beginning of the capture, as its value is slightly different from the first guess estimated for the backward propagation.

Hence, during the final few orbits, a sequence of manoeuvres need to be performed to adjust the arrival orbital elements to the desired ones. However, these manoeuvres barely change the propellant budget and they can be included in the overall orbit correction

margin of 2% on Δv. The spiral down segment for the Outreach mission is plotted in Fig. 17:
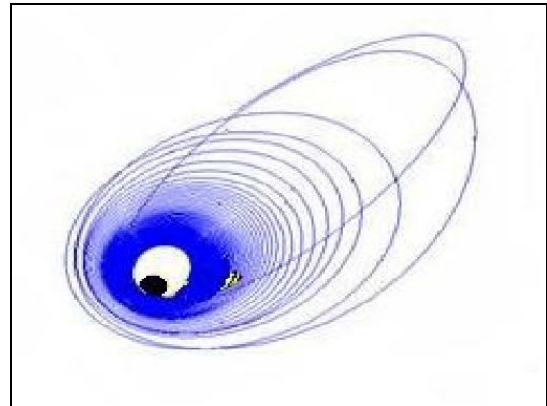

Fig. 17: Plot of the spiral-down around the Moon for the Outreach mission.

Science trajectory

The Science mission departs from the Earth on the 5th of January 2011. It takes a longer time to spiral up from the Earth due to the 11% higher launch mass than the Outreach mission. The trajectory is represented in Fig. 18:
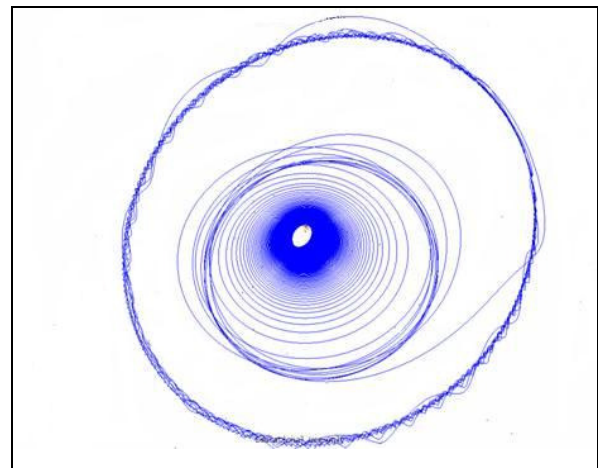

Fig. 18: Full trajectory for the Science mission projected on the plane of motion of the Earth-Moon system.

The variation of inclination and right ascension during the phasing segment are represented in Fig. 19 and Fig. 20 respectively.
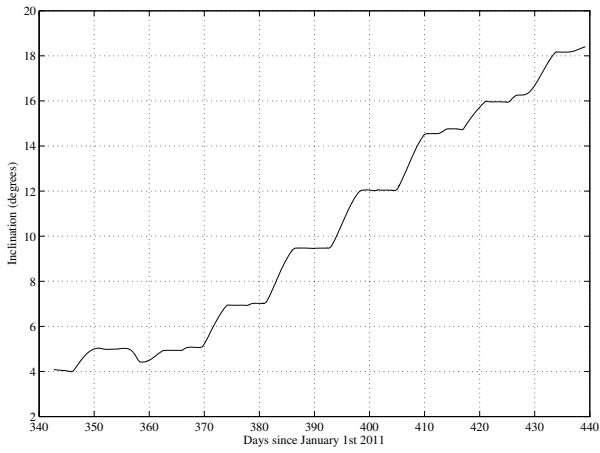
Fig. 19: Evolution of the inclination during the phasing leg for the Science mission.
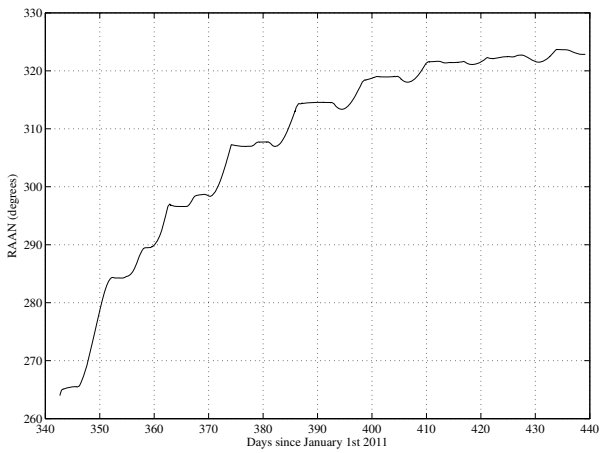

Fig. 20: Evolution of the RAAN during the phasing leg for the Science mission.

Fig. 21 contains the amplitude of the thrust vector during the phasing leg for the Science mission.
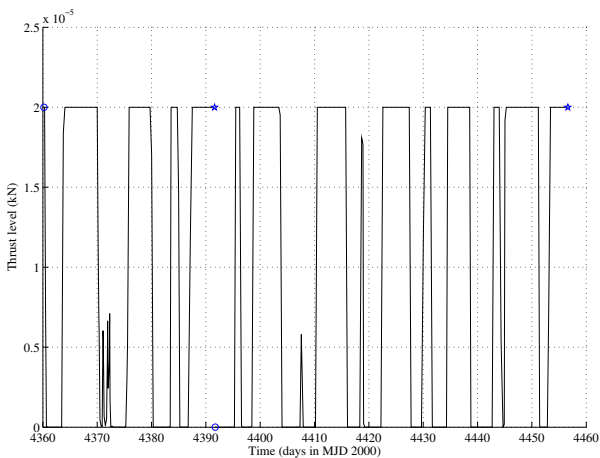

Fig. 21: Amplitude of the thrust vector during the phasing leg for the Science mission.

Fig. 22 and Fig. 23 represent the elevation and the azimuth angle of the thrust vector.
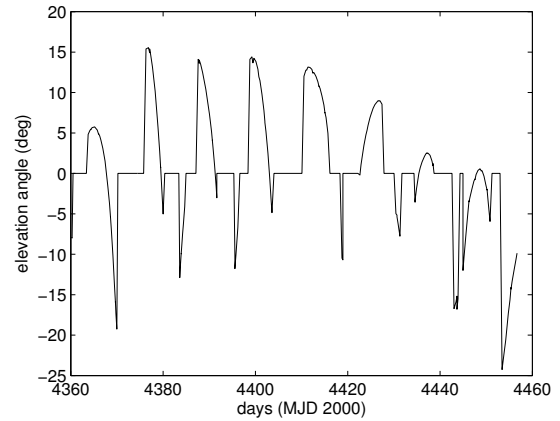

Fig. 22: Elevation angle of the thrust vector during the phasing leg for the Science mission.
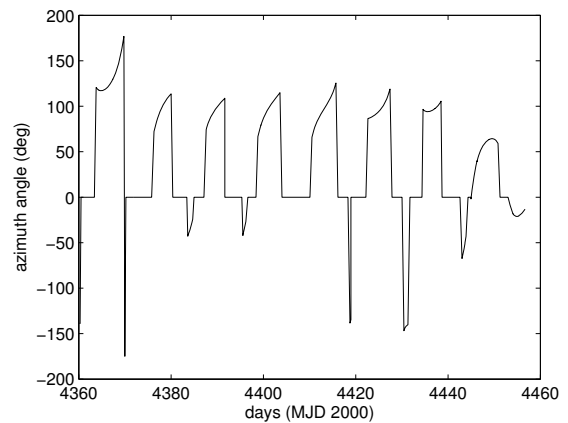

Fig. 23: Azimuth angle of the thrust vector during the phasing leg for the Science mission.

Finally Table 4 summarises the propellant budgets and the time of flight of both missions.

11

Table 4: Propellant mass, Δv budget and time of flight for Outreach and Science trajectories on the least favourable launch dates.

Phase	Outreach mission			Science mission		
	Propellant mass [kg]	*Δv [km/s]*	*Time of flight [days]*	*Propellant mass [kg]*	*Δv [km/s]*	*Time of flight [days]*
Spiralling-up phase (from GTO)	15.9	3.0	304.8	17.9	3.0	340.7
Capture phase	3.9	0.8	84.4	2.8	0.5	106.5
Spiralling-down phase (to Outreach orbit)	3.9	0.8	72.9	4.5	0.8	82.1
Spiralling-down phase (from Outreach to Science orbit)	-	-	-	2.7	0.5	119.8
Sub-Total	**23.7**	**4.5**	**462.1**	**27.9**	**4.8**	**649.1**
Orbital correction margin (5% on Δ*v*)	1.1	0.2	-	1.3	0.2	-
Additional system margin (2% on Δ*v*)	0.5	0.1	-	0.5	0.1	-
Total	**25.26**	**4.8**	**-**	**29.73**	**5.1**	**-**

3.1. *Discussion on the uncertainties regarding the worst case scenario*

Some margins were added to the Δ*v*, to take into account the approximations made in the model.

First of all, since a transfer for each launch date was not fully defined, an uncertainty on the worst case exists. Two other sources of uncertainty exist due to the ranking function and the use of a local optimiser.

For each Earth spiral chosen, a corresponding lunar spiral was selected based on the results of the ranking function in eq. (3). The ranking is designed to optimise the fuel consumption by measuring the difference between the orbital elements. In some cases however, the selected ranking may not result in the *best* orbit in terms of fuel consumption. In this rare case, the mass of the propellant is overestimated.

As a consequence, this may lead to an unrepresentative comparison when choosing the worst-case launch date by underestimating the associated propellant consumption.

To mitigate this risk, one future option would be to compare the results from other ranking functions on the Moon spirals and observe if recurrent trends occur.

The optimisation method uses a local optimiser based on an initial state vector. This first guess can bias the optimisation if multiple minima exist, identifying a local minimum instead of a globally optimal solution.

A 5% margin was added to Δ*v* to account for these possible sources of modelling errors. An additional margin of 2% of Δ*v* was added as a general overall margin for each subsystem.

4. CONCLUSION

The initial problem of assessing wide launch windows efficiently has been addressed by calculating an up-spiral for every launch opportunity and associating to it the most promising down-spiral out of a set of potential ones. Both spirals have continuous and tangential thrust profiles, so their propagation is straightforward. The portion of trajectory between the two, the phasing segment, is not explicitly calculated and optimized, but ranked for its optimality by a function based on the orbital elements at its tips. Hence a systematic way to compare a large number of transfers has been devised.

Further verifications need to be performed in order to confirm the validity of the ranking results by calculating with DITAN the

optimised transfers for dates covering wide launch windows.

Many refinements are possible when selecting the best Moon spirals. The ranking criteria are fundamental since they ensure the reliability and the efficiency of the launch window selection. The current ranking function results from essentially intuitive considerations, more sophisticated terms can be added to it.

A direction that will be investigated in the following months is the estimation of the optimal profile of the phasing segment using the technique of shaping parameters described in [23]. This approach could allow more reliable assessments of given legs, therefore favourable and unfavourable launch windows would be more accurately identified.

Furthermore, developing a systematic way to make use of resonances and flybys with the Moon can potentially reduce the propellant budget further.

The presented method can be applied to heliocentric low-thrust missions to planets, where the spacecraft is required to end up orbiting the given target planet. This method will be adopted for further studies.

ACKNOWLEDGEMENTS

REFERENCES

[1]   Walker R., ESMO Phase A Mission Requirements, 20/12/2006.

[2]   Bolland M., Curti G., Dell'Ariccia R., Forsman S., Mezzana G., Schlanbusch R., Taccoli C., Walker R., ESMO Phase A System Requirements, 10/01/2007.

[3]   Rayman, Marc D., Lehman, David H., "Deep Space One: NASA's first deep-space technology validation mission", Acta Astronautica, vol. 4, n. 4-10, 1997.

[4]   Cano J.L., Hechler M., Khan M., Pulido J., Schoenmaekers J., SMART-1 Consolidated Report on Mission Analysis, Issue 1.2, S1-ESC-RP-5506, July 16 2001.

[5]   Racca G. D, Marini A., Stagnaro L., van Doorena J., et al., "SMART-1 mission description and development status", Planetary and Space Science, 50 (2002) 1323 – 1337.

[6]   R. Jehn, S. Campagnola, D. Garcia, S. Kemble, "Low-thrust approach and gravitational capture at Mercury", Proceedings of the 18th International Symposium on Space Flight Dynamics, Munich, Germany, October 2004, p. 487.

[7]   Massari M., Bernelli-Zazzera F., "Options For Optimal Trajectory Design of a Mission To NEOS using Low-Thrust Propulsion", 14th AAS/AIAA Space Flight Mechanics Conference, 8-12 Feb 2004, 1-12.

[8]   Massari M., Bernelli-Zazzera F., Vasile M., "Trajectory Optimization for Mission to NEOs, using Low-Thrust Propulsion and Gravity Assist", 13th AAS/AIAA Space Flight Mechanics Meeting, 9-13 Feb 2003, 1-13.

[9]   Starchville T. F., "Optimal low-thrust Trajectories to Earth-Moon L2 Halo Orbits (Circular Problem)", AAS/AIAA Astrodynamics Specialist Conference, 4-7 Aug 1997.

[10] Starchville T. F., Melton R. G., "Optimal Low Thrust Trajectories to Earth-Moon L2 Halo Orbits (Circular Problem)", AAS/AIAA Astrodynamics Specialist conference, 4-7 Aug 1997.

[11] Vasile M., Bernelli-Zazzera F., "Targeting a Heliocentric Orbit Combining Low-Thrust Propulsion and Gravity Assist Manoeuvres", *Operational Research in Space & Air*, vol. 79, Book Series in Applied Optimization, Kluwer Academy Press, 2003.

[12] Conway B. A., "Efficient methods for the Determination of Optimal Low-Thrust Trajectories".

[13] Rauwolf G. A., Coverstone-Carroll V. L., "Near-Optimal Low-thrust Orbit Transfers Generated by a Genetic algorithm", *Journal of Spacecraft and*

Rockets, v. 33, n. 6, Nov-Dec 1996, 859-862.

[14] Petropoulos A. E., Longusky J. M., Vinh N. X., "Shape-Based analytic representations of Low-Thrust Trajectories for Gravity-Assist Applications" AAS 99-337, 563-581.

[15] Petropoulos A. E., Longuski J. M., "Shape-Based Algorithm for Automated Design of Low-Thrust, Gravity-Assist Trajectories", Journal of Spacecraft and Rockets, vol. 41, no. 5, September–October 2004.

[16] De Pascale P., Vasile M., "An approach to preliminary design of low-thrust multiple gravity assist trajectories".

[17] Ocampo C., Senent J., Capella A., "Low-Thrust Variable-Specific-Impulse Transfers and Guidance to Unstable Periodic Orbits", *Journal of Guidance and Control and Dynamics*, Vol. 28, No. 2, March–April 2005.

[18] Kluever C. A., and Pierson B. L., "Optimal Low-Trust Three-Dimensional Earth-Moon Trajectories", Journal of Guidance, Control, and Dynamics, Vol. 18, No. 4, 1995, pp. 830–837.

[19] Herman A. L., and Conway B. A., "Optimal, Low-Thrust, Earth–Moon Orbit Transfer," Journal of Guidance, Control, and Dynamics, Vol. 21, No. 1, 1998, pp. 141–147.

[20] Vasile M., Masarati P., Fornasari N., DITAN User Manual, version 4, September 2002.

[21] Ariane V User's Manual, Issue 4, Revision 0, November 2004.

[22] Battin R., An Introduction to the Mathematics and Methods of Astrodynamics, AIAA Education Series, 1999.

[23] De Pascale P., Vasile M., "Preliminary Design of Low-Thrust Multiple Gravity-Assist Trajectories", *Journal of Spacecraft and Rockets*, Vol. 42, Number 4, 2006, pp. 794-805.